Journal of the Arkansas Academy of Science

Volume 66 Article 20

2012

Current Range in Lightning Return Strokes

M. Hemmati
Arkansas Tech University, mhemmati@atu.edu

W. P. Childs
Arkansas Tech University

D. C. Waters
Arkansas Tech University

J. R. Christensen
Arkansas Tech University

B. C. Richard
Arkansas Tech University

Current Range in Lightning Return Strokes

M. Hemmati[1], W.P. Childs, D.C. Waters, J.R. Christensen, and B.C. Richard

[1]*Department of Physical Science, Arkansas Tech University, Russellville, AR 72801*

[1]Correspondence: mhemmati@atu.edu

Abstract

In our investigation of breakdown waves, we use a one-dimensional, steady-state, constant velocity fluid model. This investigation involves breakdown waves for which the electric field force on electrons is in the opposite direction of wave propagation. The waves are considered to be shock fronted and the electron gas partial pressure is large enough to sustain the wave propagation. Our basic set of electron fluid-dynamical equations is composed of the equations for conservation of mass, momentum and energy, coupled with Poisson's equation. This investigation involves breakdown waves for which a large current exists behind the shock front. The current behind the shock front alters the set of electron fluid-dynamical equations as well as the boundary conditions at the shock front. For the range of reported experimental current values (Wang et al. 1999), we have been able to solve the electron fluid dynamical equations within the dynamical transition region of the wave. Wave profile for electric field and electron velocity, number density and temperature within the dynamical transition region of the wave will be presented.

Introduction

In the case of breakdown waves in a long discharge tube, near the electrode where the potential gradient in the gas is greatest, a small quantity of gas is ionized. Analysis of the spectrum of radiation emitted from electric breakdown of a gas reveals no Doppler shift, indicating that the ions have negligible motion. The large difference in mobilities of positive ions and electrons causes establishment of a space charge and consequently a space charge field. The electric field accelerates the free electrons until they acquire enough energy for collisional ionization of the gas. Since the ionized gas is a conductor and it cannot hold internal electric filed, the electric field which has its maximum value at the interface between the ionized gas and the neutral gas has to reduce to a negligible value at the trailing edge of the wave. The wave propagates with a speed close to the speed of light, with a wave front discontinuity, which obeys a Rankin-Hugoniot type condition on the electron fluid.

We are considering waves for which the direction of the electric field is such that the net electric field force on electrons causes an electron mobility motion opposite to the direction of wave advance. Such waves are referred to as antiforce waves. In the case of antiforce waves (lightning return stroke), the electron temperature, and therefore the electron gas pressure is large enough to counter this force and provide the net force responsible for the wave propagation. A model of return stroke in lightning, for example, might consist of a wave for which a large current exists behind the wave front.

Following the shock front is a thin region in which the electric field and electron velocity are changing rapidly, while the changes in electron temperature and electron number density are not so rapid. This region is referred to as the sheath region. In the sheath region, the electric field starting with its maximum value at the shock front reduces to a negligible value at the end of the sheath and the electrons slow down to speeds comparable to those of heavy particles and ions. The sheath region of the wave is followed by a relatively thicker region in which the electric field and electron velocity are zero, while the electron temperature and number density are changing. This region is referred to as the quasi-neutral region. In the quasi-neutral region, the electron gas cools down by further ionization of the heavy particles.

Model

In our fluid model, in laboratory frame where the heavy particles are considered to be at rest, a plane wave is propagating in the positive x direction with speed V_0. Therefore, in a frame where the wave front is stationary at $x = 0$, the wave extends from $x = 0$ to $x = -\infty$, and the plane $x = 0$ divides the neutral gas in front of the wave from the three component gas composed of electrons, ions and neutral particles behind the wave front.

Because of unknowns in experimental studies, it is difficult to directly compare experimental results with computational results from our fluid-model application. However, our results agree with many other theoretical studies and experimental results.

For theoretical investigation of breakdown wave, we will use the equations that were developed by Fowler et al. (1984) and represent a one-dimensional, steady-state, constant velocity electron fluid-dynamical wave propagating into a neutral medium. This set of electron fluid-dynamical equations consists of the equations of conservation of mass, momentum, and energy coupled with Poisson's equation:

$$\frac{d(n\upsilon)}{dx} = n\beta, \qquad [1]$$

$$\frac{d}{dx}[mnv(\upsilon - V) + nkT_e] = -enE - Kmn(\upsilon - V), \qquad [2]$$

$$\frac{d}{dx}[mn\upsilon(\upsilon - V)^2 + nkT_e(5\upsilon - 2V) + 2en\upsilon\Phi - \frac{5nk^2T_e}{mK}\frac{dT_e}{dx}]$$

$$= -3(\frac{m}{M})nkKT_e - (\frac{m}{M})Kmn(\upsilon - V)^2, \qquad [3]$$

$$\frac{dE}{dx} = \frac{e}{\varepsilon_0}n(\frac{v}{V} - 1). \qquad [4]$$

where n, v, T_e, e and m represent the electron number density, velocity, temperature, charge, and mass, respectively, and $M, E, E_0, V, k, K, x, \beta,$ and ϕ represent the neutral particle mass, electric field within the sheath region, electric field at the wave front, wave velocity, Boltzmann's constant, elastic collision frequency, position within the sheath region, ionization frequency and ionization potential of the gas.

To reduce the set of electron fluid dynamical equations to a non-dimensional form, Fowler et al. (1984) introduced the following dimensionless variables:

$$\eta = \frac{E}{E_o}, \nu = (\frac{2e\phi}{\varepsilon_o E_o^2})n, \psi = \frac{v}{V}, \theta = \frac{T_e k}{2e\phi}, \xi = \frac{eE_b x}{mV^2},$$

$$\alpha = \frac{2e\phi}{mV^2}, \kappa = \frac{mV}{eE_o}K, \mu = \frac{\beta}{K}, \omega = \frac{2m}{M},$$

in which $\eta, \nu, \psi, \theta, \mu,$ and ξ represent the dimensionless net electric field of the applied field plus the space charge field, electron number density, electron velocity, electron gas temperature, ionization rate, and position within the sheath region, while α and κ represent wave parameters. These dimensionless variables are then substituted into equations 1, 2, 3 and 4, yielding

$$\frac{d(\nu\psi)}{d\xi} = \kappa\mu\nu, \qquad [5]$$

$$\frac{d}{d\xi}[\nu\psi(\psi - 1) + \alpha\nu\theta] = -\nu\eta - \kappa\nu(\psi - 1), \qquad [6]$$

$$\frac{d}{d\xi}[\nu\psi(\psi - 1)^2 + \alpha\nu\theta(5\psi - 2) + \alpha\nu\psi + \alpha\eta^2 - \frac{5\alpha^2\nu\theta}{\kappa}\frac{d\theta}{d\xi}] = -\omega\kappa\nu[3\alpha\theta + (\psi - 1)^2], \qquad [7]$$

$$\frac{d\eta}{d\xi} = \frac{\nu}{\alpha}(\psi - 1). \qquad [8]$$

In solving the antiforce case problem, in which all quantities including κ are positive and ξ is positive backward, we will use the set of non-dimensional variables introduced by Hemmati (1999).

$$\eta = \frac{E}{E_o}, \nu = (\frac{2e\phi}{\varepsilon_o E_o^2})n, \psi = \frac{v}{V}, \theta = \frac{T_e k}{2e\phi}, \xi = -\frac{eE_o x}{mV^2},$$

$$\alpha = \frac{2e\phi}{mV^2}, \kappa = -\frac{mV}{eE_o}K, \mu = \frac{\beta}{K}, \omega = \frac{2m}{M}.$$

For current bearing antiforce waves, we will also use Hemmati et al.'s (2011) modified set of electron fluid dynamical equations. In non-dimensional form, their electron fluid dynamical equations are

$$\frac{d}{d\xi}[\nu\psi] = \kappa\mu\nu, \qquad [9]$$

$$\frac{d}{d\xi}[\nu\psi(\psi - 1) + \alpha\nu\theta] = \nu\eta - \kappa\nu(\psi - 1), \qquad [10]$$

$$\frac{d}{d\xi}[\nu\psi(\psi - 1)^2 + \alpha\nu\theta(5\psi - 2) + \alpha\nu\psi - \frac{5\alpha^2\nu\theta}{\kappa}\frac{d\theta}{d\xi} + \alpha\eta^2] = 2\eta\kappa\iota\alpha - \omega\kappa\nu[3\alpha\theta + (\psi - 1)^2], \qquad [11]$$

$$\frac{d\eta}{d\xi} = \kappa\iota - \frac{\nu}{\alpha}(\psi - 1). \qquad [12]$$

Where, ι, is the dimensionless current and is related to the current behind the wave front, I_1, by the equation $\iota = I_1 / \varepsilon_0 K E_0$.

Earlier theoretical investigations of breakdown waves considered the ionization rate within the sheath region of the wave to be constant, or to be a function of temperature only. However, in 1983, Fowler (1983) showed that the assumption of a constant ionization rate was incorrect and therefore replaced it by a computation that was based on free trajectory theory. Fowler's (1983) computation included ionization from both random and directed electron motions within the sheath region of the wave. For ionization in a strong electric field with independent electron drift velocity, Fowler (1983) derived an equation for ionization rate, and in non-dimensional form it is given by the following function

$$\mu = \mu_o \int_{1/\sqrt{2\theta}}^{\infty} \sigma_i z^2 dz \int_B^{\infty} \frac{e^{-(z-u)^2} - e^{-(z+u)^2}}{u} du\, e^{-2Cu}, \quad [13]$$

where $B = (1-\psi)/\sqrt{2\alpha\theta}$ and $C = \kappa\sqrt{2\alpha\theta}/\eta$. This function, which changes from accelerational ionization at the front of the wave to directed velocity ionization in the intermediate stages of the wave, to thermal ionization at the end of the wave, in the case of breakdown waves moving with a slow speed, does remain considerably constant at the beginning of the sheath; however, as one traverses through the sheath, the ionization rate changes.

Results and Discussion

Performing a statistical study on the initial stage of negative rocket-triggered lightning using 37 channel-base current recordings, Wang et al. (1999) reported average currents in an individual lightning discharge to vary from a minimum of 27 A to a maximum of 316 A. Their upward positive leader is followed by a pulse with a typical current peak of about 1 kA. In an approach based on antenna theory to describe the lightning return stroke, Moini et al. (2000) approximated the lightning channel by a straight and vertical monopole antenna above a perfectly conducting ground. The antenna is fed at its lower end by a voltage source such that the antenna input current, which represents the lightning return-stroke current at the lightning channel base, can be specified. They compare their model to four commonly used "engineering" return-stroke models, and find reasonably good agreement. Using a channel-base current waveform for comparison of different models, Moini et al. (2000) reported a peak current of 11 kA. Comparing five return-stroke models, each allowing the use of measured channel-base current and return-stroke speed as inputs for the computation of channel current distribution and remote electric field, Thottappillil and Uman (1993) report a return stroke starting from the ground with a speed of 3.5×10^7 m/s and increasing exponentially to the measured return stroke speed of 1.2×10^8 m/s within a distance of 55 m. In the same study, the current waveforms of return strokes have a slowly rising ramp at the beginning, with a maximum current value of approximately 5 kA at the end of the ramp. However, they report current peak values ranging from 8 kA to 25 kA.

Determining the ratio of the elastic collision frequency, K (McDaniel 1964), to the electron gas pressure, P, gives $K/P = 3x10^8$ for helium and $K/P = 4.8x10^7$ for nitrogen at 273 K. At a temperature of 10^5, K will be $2.4x10^9$ for helium and $9x10^9$ for nitrogen and applied fields are usually of order $10^5 V/m$. Considering that E_0, K, β in our formulas are scaled with P (the electron gas pressure) and using the values of $I_1, \varepsilon_0, E_0, K$ one can estimate the value of ι, which is of order one.

A trial-and-error method was utilized to integrate equations 9 through 12. For a given wave speed, α, a set of values for wave constant, κ, electron velocity, ψ_1, and electron number density, ν_1, at the wave front were chosen. The values of κ, ψ_1 and ν_1 were repeatedly changed in integrating equations 9 through 12 until the process lead to a conclusion in agreement with the expected conditions at the end of the dynamical transition region of the wave

$$\left[\eta_2 \to 0,\ \ \psi_2 \to 1,\ \ \left(\frac{d\eta}{d\xi}\right)_2 \to 0,\ \ \left(\frac{d\psi}{d\xi}\right)_2 \to 0\right]. \quad [14]$$

For α = 0.01, 0.05 and 0.1 and $\iota = 0.7$, we have been able to integrate the set of electron fluid dynamical equations (equations 9-12), through the sheath region of the wave. Our solutions meet the

conditions described by equation 14 at the trailing edge of the wave. α = 0.01, 0.05 and 0.1 represent wave speeds of $3x10^7\, m/s$, $1.33x10^7\, m/s$ and $0.937x10^7\, m/s$, respectively, and conform with the lower experimental speed range for the return-stroke of lightning. The successful solutions required the following boundary values

$$\alpha = 0.01, \kappa = 1.3, \psi_1 = 0.6564, \nu_1 = 0.88$$
$$\alpha = 0.05, \kappa = 0.6, \psi_1 = 0.826, \nu_1 = 0.9289$$
$$\alpha = 0.1, \kappa = 0.44, \psi_1 = 0.678, \nu_1 = 0.8889$$

Figure 1 shows a graph of the dimensionless electric field, η, as a function of electron velocity, ψ, within the sheath region of the wave. The dimensionless electron velocity at the shock front is a number between 0 and 1; therefore, as one can see from the Poisson's equation (equation 12), the electric field initially should increase until the dimensionless electron velocity becomes larger than 1. As one traverses through the sheath region, the electric field decreases to a negligible value, while the electrons slow down to speeds comparable to those of heavy particles at the end of the sheath region ($\eta_2 \to 0, \psi_2 \to 1$).

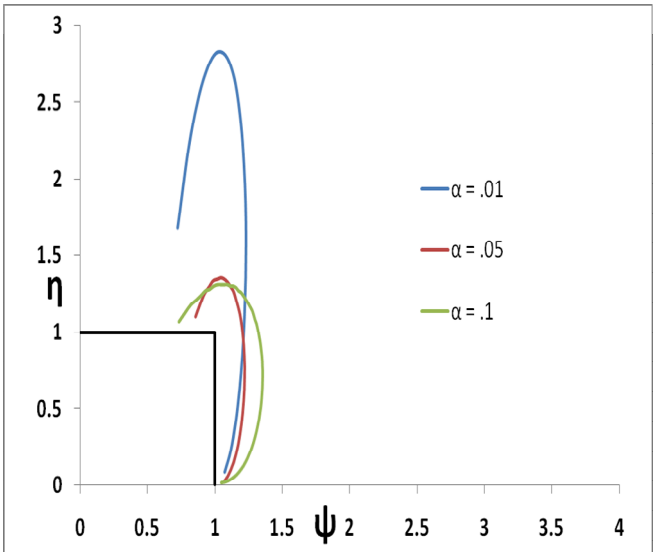

Figure 1. Electric field, η, as a function of electron velocity, ψ, within the sheath region of current bearing antiforce waves for alpha values of .01, .05, and 0.1 with current value of 0.7.

Figure 1 shows that for all three speed values, the solutions meet the expected conditions at the end of the sheath region. Figure 2 is a graph of the dimensionless electric field, η, as a function of dimensionless position, ξ, within the sheath region of the wave. The graph shows that as α increases (wave speed decreases), the sheath thickness increases as well. As sheath thickness increases, integration of the set of equations become more difficult and time consuming.

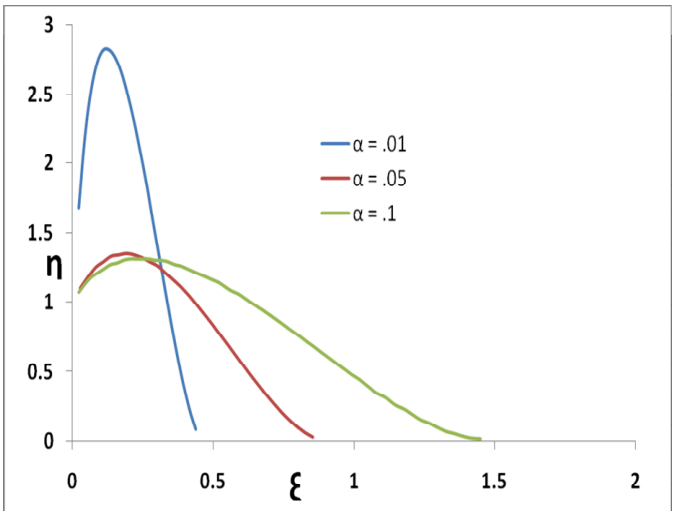

Figure 2. Electric field, η, as a function of position, ξ, within the sheath region of current bearing antiforcewaves for alpha values of .01, .05, and 0.1 with current value of 0.7.

The wave with α = 0.01 has a relatively smaller sheath thickness, and the dimensionless sheath thickness value of $\xi = 0.5$, represents an actual sheath thickness of 2.5 cm. Studying the structure of the antiforce electron fluid dynamical plane waves, Sanmman and Fowler (1975) report that the field attains its maximum value fairly quickly at 0.041 m behind the wave front, and then, it gradually decreases over a large distance. However, in their study of electron density measurments behind strong shock waves, Fujita et al. (2003) report an average wave thickness of 5 cm. Our sheath thicness values compare well with those reported by Sanmann and Fujita.

Figure 3 depicts the dimensionless electron velocity, ψ, as a function of dimensionless position, ξ, within the sheath region. For all three wave speeds, the dimensionless electron velocity initially increases; however, after reaching its peak value inside the

sheath, it starts decreasing and reduces to 1 at the trailing edge of the wave.

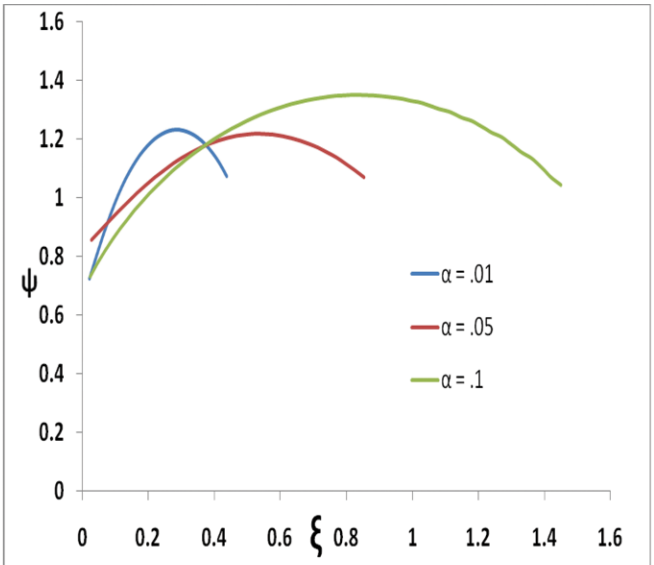

Figure 3. Electron velocity, ψ, as a function of position, ξ, within the sheath region of current bearing antiforce waves for alpha values of .01, .05, and 0.1 with current value of 0.7

Figure 4 shows the dimensionless electron temperature, θ, as a function of dimensionless position, ξ, within the sheath region of the wave. The figure shows that as the wave speed decreases (α value increases) the temperature within the sheath region decreases as well. However, for all three wave speeds, starting from a relatively smaller temperature behind the shock front, the temperature gradually increases and reaches its maximum value at the end of the sheath. The maximum dimensionless temperature of 65 for $\alpha = 0.01$, represents an actual temperature of $3.77x10^7 K$. Applying fluid dynamics techniques to the passage of ionizing waves counter to strong electric fields, for a wave speed value of $10^7 m/s$, Sanmann and Fowler (1975) report that the electron temperature increases very rapidly behind the wave front until it reaches its peak value of $3.17x10^7 K$ at a distance of 5.4 cm behind the wave front. Our maximum temperature value of $3.77x10^7 K$ $(\theta = 65)$, for a higher wave speed value of $3x10^7 m/s$, compares well with the temperature value reported by Sanmann and Fowler (1975).

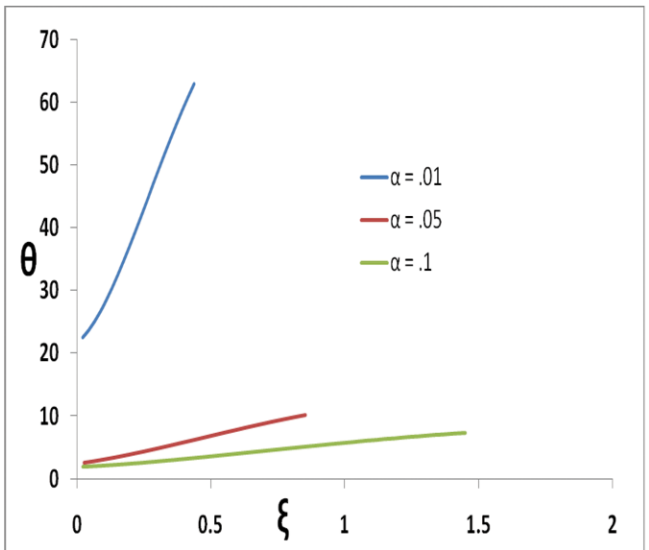

Figure 4. Electron temperature, θ, as a function of position, ξ, within the sheath region of current bearing antiforce waves for alpha values of .01, .05, and 0.1 with current value 0.7.

For a dimensionless current value of $\iota = 0.7$, figure 5 shows electron number density, ν, as a function of dimensionless position, ξ, for three different values of wave speeds. As one traverses through the wave, for all three wave speeds, the electron number density initially decreases, and then, increases and reaches its maximum value at the end of the sheath region.

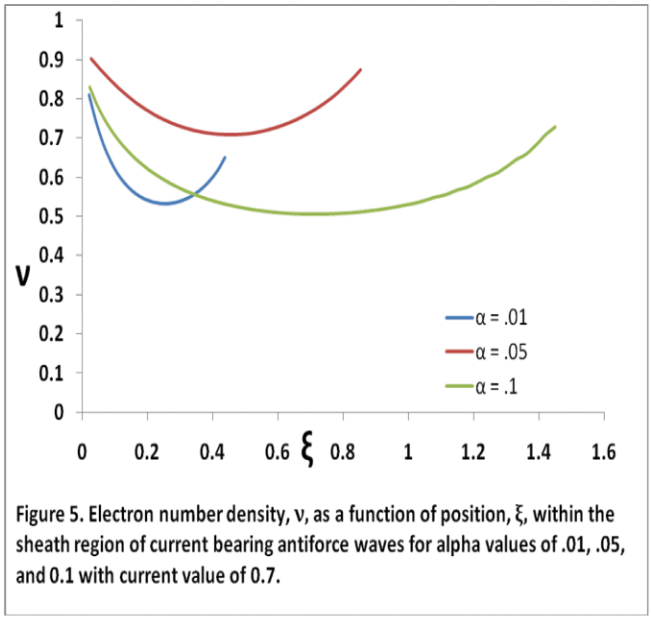

Figure 5. Electron number density, ν, as a function of position, ξ, within the sheath region of current bearing antiforce waves for alpha values of .01, .05, and 0.1 with current value of 0.7.

Our average dimensionless electron number density of 0.7 represents an actual electron number density of $7.7x10^{15}/m^3$. In their model study of propagation of ionizing wave during breakdown in a straight tube containing argon, Brok et al. (2003) reported a peak electron number density of $4x10^{15}/m^3$, which compares well with our electron number density. Studying the effect of electron number density on shock wave propagation in optically pumped plasmas, White et al. (2002) reported an electron number density of $9x10^{15}/m^3$.

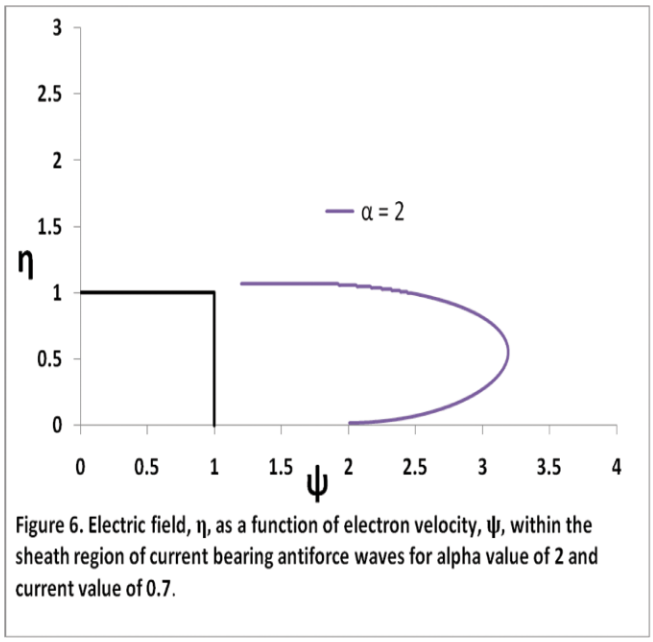

Figure 6. Electric field, η, as a function of electron velocity, ψ, within the sheath region of current bearing antiforce waves for alpha value of 2 and current value of 0.7.

For the dimensionless current value of 0.7, we also attempted to integrate the electron fluid dynamical equations for $\alpha = 2$. The integration process was very time consuming. Our best result required the following values for the wave constant, κ, and the dimensionless electron velocity and electron number density at the wave front $(\alpha = 2, \kappa = 0.1, \psi_1 = 0.61, \nu_1 = 0.61)$. For $\alpha = 2$, figures 6 and 7 respectively depict dimensionless electric field, η, as a function of dimensionless electron velocity, ψ, and the dimensionless electron velocity, ψ, as a function of dimensionless position, ξ, within the sheath region of the wave. As the graphs indicate, even our best result failed to meet the expected physical conditions at the training edge of the wave. Therefore, for dimensionless current of 0.7, $\alpha = 2$ $(V = 2.1x10^6 m/s)$ seems to be the lowest wave velocity for which solutions of the set of electron fluid dynamical equations become possible.

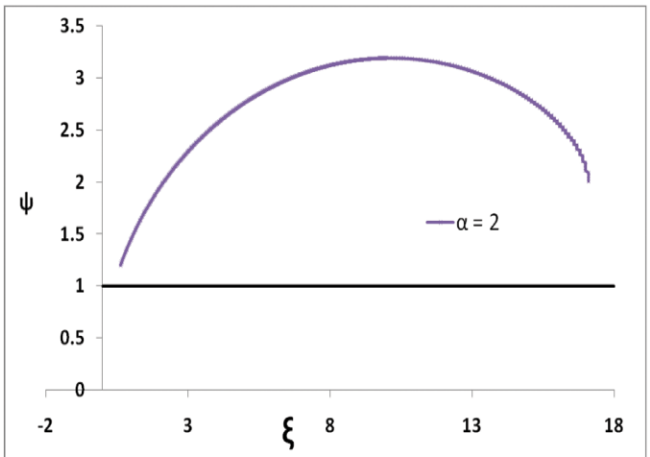

Figure 7. Electron velocity, ψ, as a function of position, ξ, within the sheath region of current bearing antiforce waves for alpha value of 2 and current value of 0.7.

For $\alpha = 0.05$, we also attempted to integrate the electron fluid dynamical equations for larger current values. As we increased the dimensionless current value, integration of the set of equations became more difficult. However, solutions for current values below 4 were possible. Figures 8 and 9 respectively show the dimensionless electric field, η, as a function of electron velocity, ψ, and the dimensionless electron velocity, ψ, as a function of position, ξ, within the sheath region of the wave for our best solution for $\iota = 4$. The required values for dimensionless electron velocity and electron number density at the shock front were

$$\alpha = 0.05, \kappa = 0.6, \psi_1 = 0.7515, \nu_1 = 0.81.$$

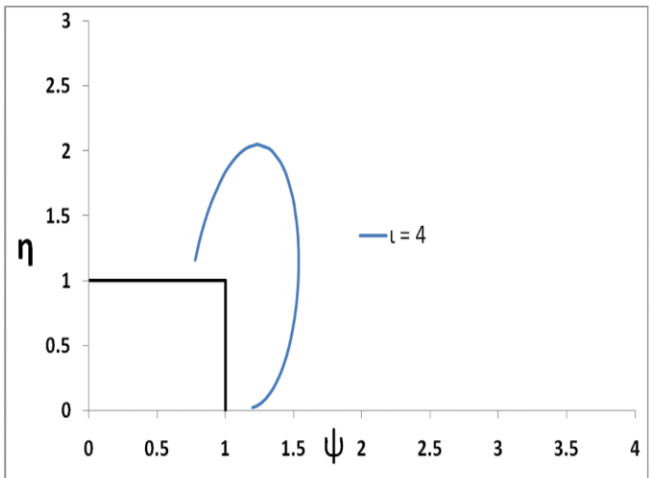

Figure 8. Electric field, η, as a function of electron velocity, ψ, within the sheath region of current bearing antiforce waves for alpha value of .05 and current value of 4.

As Figures 8 and 9 indicate, the electric field and electron velocity values do not meet the expected conditions at the end of the sheath region. Therefore, for $\alpha = 0.05$, $\iota = 4$ seems to be the cut-off point for which solutions of the set of electron fluid dynamical equations become possible.

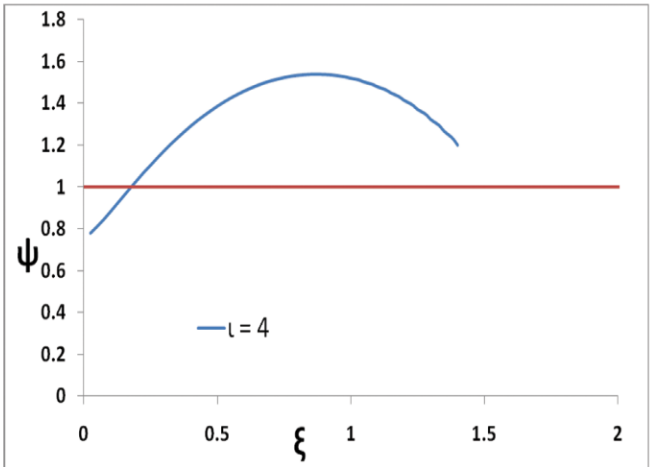

Figure 9. Electron velocity, ψ, as a function of position, ξ, within the sheath region of current bearing antiforce waves for alpha value of .05 and current value of 4.

Conclusions

For current-bearing antiforce waves, integration of the set of electron fluid dynamical equations (equations 9-12) through the sheath region of the wave for speed and current values comparable with the experimentally measured values has been successful. This confirms the validity of our modified set of electron fluid dynamical equations and our fluid model. Even if due to the time limitation we have not been able to determine the exact range of speed and current values for which solutions to our equations become possible, it seems there might be current and speed ranges similar to those measured experimentally.

Acknowledgment

The authors would like to express gratitude for the financial support provided by the Arkansas Space Grant Consortium.

Literature Cited

Brok WJM, **J van Dijk**, **MD Bowden**, **JJAM van der Mullen** and **GMW Kroesen**. 2003. A model study of propagation of the first ionization wave during breakdown in a straight tube containing argon. Journal of Physics D: Applied Physics 36:1967-79.

Fowler RG. 1983. A trajectory theory of ionization in strong electric fields. Journal of Physics B: Atomic and Molecular Physics 16:4495-4510.

Fowler RG, **M Hemmati**, **RP Scott** and **S Parsenajadh**. 1984. Electric breakdown waves: Exact numerical solutions. Part I. The Physics of Fluids 27(6):1521-1526.

Fujita K, **S Sato** and **T Abe.** 2003. Electron density measurements behind shock waves by $H-\beta$ profile matching. Journal of Thermodynamics and Heat Transfer 17:210-6.

Hemmati M. 1999. Electron shock waves: speed range for antiforce waves. Proc. 22nd International Symposium on Shock Waves (ISSW22); July 18-23, 1999; Imperial College, London, UK. 2:995-1000.

Hemmati M, **WP Childs**, **JD Counts** and **DC Waters**. 2011. Antiforce current bearing waves. Proc. 28th International Symposium on Shock Waves (ISSW28), July 2011, England.

McDaniel EW. 1964. Collision phenomena in ionized gases. Wiley, New York.

Moini R, **B Kordi**, **G Rafi** and **VA Rakov**. 2000. A new lightning return stroke model based on antenna theory. Journal of Geophysical Research 105 (D24):29693-29702.

Sanmann E and **RG Fowler**. 1975. Structure of electron fluid dynamical plane waves: antiforce waves. The Physics of Fluides 18(11):1433-8.

Thottappillil R and **M Uman**. 1993. Comparison of lightning return-stroke models. Journal of Geophysical Research 98(D12):22903-22914.

Wang D, **VA Rakov**, **MA Uman**, **MI Fernandez**, **KJ Rambo**, **GH Schnetzer** and **RJ Fisher**. 1999. Characterization of the initial stage of negative rocket-triggered lightning. Journal of Geophysical Research 104(D4):4213-4222.

White AR, **P Palm**, **E Plonjes**, **VV Subramaniam** and **IV Adamovich**. 2002. Effect of electron density on shock wave propagation in optically pumped plasmas. Journal of Applied Physics 91(5):2604-2610.